Preprint typeset in JHEP style - HYPER VERSION

Likelihood analysis of the next-to-minimal supergravity motivated model

Csaba Balázs

School of Physics, Monash University, Melbourne Victoria 3800, Australia
E-mail: csaba.balazs@sci.monash.edu.au

Daniel Carter

School of Physics, Monash University, Melbourne Victoria 3800, Australia
E-mail: daniel.carter@sci.monash.edu.au

Abstract: In anticipation of data from the Large Hadron Collider (LHC) and the potential discovery of supersymmetry, in this work we seek an answer to the following: What are the chances that supersymmetry will be found at the LHC? Will the LHC data be enough to discover a given supersymmetric model? And what other measurements can assist the LHC establish the presence of supersymmetry? As a step toward answering these general questions, we calculate the odds of the next-to-minimal version of the popular supergravity motivated model (NmSuGra) being discovered at the LHC to be 4:3 (57 %). We also demonstrate that viable regions of the NmSuGra parameter space outside the LHC reach can be covered by upgraded versions of dark matter direct detection experiments, such as super-CDMS, at 99 % confidence level. Due to the similarities of the models, we expect very similar results for the constrained minimal supersymmetric standard model (CMSSM).

Keywords: Supersymmetry; Collider phenomenology; Dark matter; Rare decays; Electroweak precision experiments..

Contents

1. Introduction

Supersymmetry is one of the most robust theories that can solve outstanding problems of the standard model (SM) of elementary particles. The theory naturally explains the dynamics of electroweak symmetry breaking while preserving the hierarchy of fundamental energy scales. It also readily accommodates dark matter, the asymmetry between baryons and anti-baryons, the unification of gauge forces, gravity, and more. But if supersymmetry is the solution to the problems of the standard model, then its natural scale is the electroweak scale, and it is expected to be observed in upcoming experiments, most notably the CERN Large Hadron Collider (LHC). In this work, we will attempt to determine, quantitatively, what the chances are that this may occur for the simplified case of a constrained supersymmetric model.

One of the main motivations for supersymmetry is that it can naturally bridge the hierarchy between the weak and Planck scales. Unfortunately, the presence of the superpotential μ term in the minimal supersymmetric extension of the standard model (MSSM) undermines this very aim [1]. Experimental data have also squeezed the MSSM into fine-tuned regions, creating the supersymmetric little hierarchy problem[2]. Extensions of the MSSM by gauge singlet superfields not only resolve the μ problem, but can also ameliorate the little hierarchy problem [3, 4, 5]. In the next-to-minimal MSSM (NMSSM), the μ term is dynamically generated and no dimensionful parameters are introduced in the superpotential (other than the vacuum expectation values that are all naturally weak scale), making the NMSSM a truly natural model [6, 7, 8, 9, 10, 11, 12, 13, 14, 15, 16, 17, 18, 19, 20, 21, 22, 23].

Over the last two decades, due to its simplicity and elegance, the constrained MSSM (CMSSM) and the minimal supergravity-motivated (mSuGra) model became a standard in supersymmetry phenomenology. Guided by this, within the NMSSM, we impose the universality of sparticle masses, gaugino masses, and tri-linear couplings at the grand unification theory (GUT) scale, thereby defining the next-to-minimal supergravity-motivated (NmSuGra) model. This approach ensures that all dimensionful parameters of the NMSSM scalar potential also naturally arise from supersymmetry breaking in a minimal fashion. NmSuGra also reduces the electroweak and dark matter fine-tunings of mSuGra.

Using a Bayesian likelihood analysis, we identify the regions in the parameter space of the NmSuGra model that are preferred by the present experimental limits from various collider, astrophysical, and low-energy measurements. We combine theoretical exclusions with experimental limits from the CERN Large Electron-Positron (LEP) collider, the Fermilab Tevatron, NASA's Wilkinson Microwave Anisotropy Probe (WMAP) satellite (and other related astrophysical measurements), the Soudan Cryogenic Dark Matter Search (CDMS), the Brookhaven Muon g−2 Experiment, and various b-physics measurements including the rare decay branching fractions $b \to s\gamma$ and $B_s \to l^+l^-$. Thus we show that, given current experimental constraints, the favored parameter space can be detected by a combination of the LHC and an upgraded CDMS at the 95 % confidence level.

In the next section we define the next-to-minimal version of the supergravity motivated model (NmSuGra). Then, in Section 3, we summarize the main concepts of Bayesian inference that we use in this work. Section 4 contains the numerical results of our likelihood analysis, and Section 5 gives the outlook for the experimental detection of NmSuGra.

2. The next-to-minimal supergravity motivated model

The next-to-minimal supersymmetric model (NMSSM) is defined by the superpotential

$$W_{NMSSM} = W_{MSSM}|_{\mu=0} + \lambda \hat{S}\hat{H}_u \cdot \hat{H}_d + \frac{\kappa}{3}\hat{S}^3, \tag{2.1}$$

where

$$W_{MSSM}|_{\mu=0} = y_t \hat{Q}_L \cdot \hat{H}_u \hat{T}^c_R - y_b \hat{Q}_L \cdot \hat{H}_d \hat{B}^c_R - y_\tau \hat{L}_L \cdot \hat{H}_d \hat{L}^c_R \tag{2.2}$$

is the MSSM superpotential containing only Yukawa terms and having μ set to zero [24]. The left (right) handed matter superfields $\hat{Q}_L$, $\hat{L}_L$ ($\hat{T}_R$, $\hat{B}_R$, $\hat{L}_R$), and Higgs $\hat{H}_{u,d}$ superfields are $SU(2)_L$ doublets (singlets), while $\hat{S}$ is a standard gauge singlet. The couplings λ, κ, and y_i are dimensionless, and $\hat{X} \cdot \hat{Y} = \epsilon_{\alpha\beta}\hat{X}^\alpha \hat{Y}^\beta$ with the fully antisymmetric tensor normalized as $\epsilon_{11} = 1$. The corresponding soft supersymmetry breaking terms are

$$\mathcal{L}^{soft}_{NMSSM} = \mathcal{L}^{soft}_{MSSM}|_{B=0} - M_S^2|\tilde{S}|^2 - (\lambda A_\lambda \tilde{S} H_u \cdot H_d + \frac{\kappa A_\kappa}{3}\tilde{S}^3 + h.c.). \tag{2.3}$$

Here

$$\mathcal{L}^{soft}_{MSSM}|_{B=0} = \mathcal{L}^{soft}_{gaugino} + \mathcal{L}^{soft}_{scalar} + \mathcal{L}^{soft}_{tri-linear}, \tag{2.4}$$

contains the mass terms for the twelve gauginos ($i = 1...3$, $a = 1...8$)

$$\mathcal{L}^{soft}_{gaugino} = -\frac{1}{2}(M_1 \bar{\tilde{B}}\tilde{B} + M_2 \bar{\tilde{W}}_i \tilde{W}_i + M_3 \bar{\tilde{G}}_a \tilde{G}_a + h.c), \tag{2.5}$$

the sfermions and Higgses

$$\begin{aligned}\mathcal{L}^{soft}_{scalar} = -\ (\ & M^2_{\tilde{Q}}|\tilde{Q}|^2 + M^2_{\tilde{T}_R}|\tilde{T}_R|^2 + M^2_{\tilde{B}_R}|\tilde{B}_R|^2 + M^2_{\tilde{L}}|\tilde{L}|^2 + M^2_{\tilde{L}_R}|\tilde{L}_R|^2 + \\ & M^2_{H_u}|H_u|^2 + M^2_{H_d}|H_d|^2),\end{aligned} \tag{2.6}$$

and the soft tri-linear terms

$$\mathcal{L}^{soft}_{tri-linear} = -(y_t A_t \tilde{Q} \cdot H_u \tilde{T}^c_R - y_b A_b \tilde{Q} \cdot H_d \tilde{B}^c_R - y_\tau A_\tau \tilde{L} \cdot H_d \tilde{L}^c_R + h.c.). \tag{2.7}$$

The NMSSM superpotential possesses a global Z_3 symmetry which is broken during the electroweak phase transition in the early universe. The resulting domain walls should disappear before nucleosynthesis. However Z_3 breaking (via singlet tadpoles) leads to a vacuum expectation value (vev) for the singlet that is much larger than the electroweak scale. Thus the requirement of the fast disappearance of the domain walls appears to destabilize the hierarchy of vevs in the NMSSM. Fortunately, in Ref.s [25, 26] is was shown that, by imposing a Z_2 R-symmetry, both the domain wall and the stability problems can be eliminated. Following [25], we assume that tadpoles are induced, but they are small and their effect on the phenomenology is negligible.

We use supergravity motivated boundary conditions to parametrize the soft masses and tri-linear couplings. Defining a constrained version of the NMSSM, we assume unification of the gaugino masses

$$M_1 = M_2 = M_3 = M_{1/2}, \tag{2.8}$$

the sfermion and Higgs masses (but not the singlet mass)

$$M^2_{\tilde{Q}} = M^2_{\tilde{T}_R} = M^2_{\tilde{B}_R} = M^2_{\tilde{L}} = M^2_{\tilde{L}_R} = M^2_{H_u} = M^2_{H_d} = M^2_0, \tag{2.9}$$

and the tri-linear couplings

$$A_t = A_b = A_\tau = A_\kappa = A_\lambda = A_0, \tag{2.10}$$

at the scale of a grand unified theory (GUT) where the three standard gauge couplings meet $g_1 = g_2 = g_3 = g_{GUT}$. This leaves six parameters in the model: M_0, $M_{1/2}$, A_0, M_S, λ and κ. Electroweak symmetry breaking introduces the Higgs and singlet vevs, $\langle H_u \rangle$, $\langle H_d \rangle$, $\langle S \rangle$. From Eq.2.1 we see that when the singlet acquires a vev, the MSSM μ term is dynamically generated as $\mu = \lambda \langle S \rangle$, and thus the NMSSM naturally solves the μ problem. The three minimization equations for the Higgs potential [27] and

$$\langle H_u \rangle^2 + \langle H_d \rangle^2 = v^2 \tag{2.11}$$

(here $v = \sqrt{2}/g_2$ is the standard Higgs vev) eliminate four parameters. Thus our constrained NMSSM model has only five free parameters and a sign. Defining $\tan\beta =$

$\langle H_u \rangle / \langle H_d \rangle$, the parameters of the next-to-minimal supergravity motivated model (NmSuGra) are

$$P = \{M_0, M_{1/2}, A_0, \tan\beta, \lambda, \mathrm{sign}(\mu)\}. \tag{2.12}$$

Constrained versions of the NMSSM have been studied in the recent literature. The most constrained version is the cNMSSM [28] with $M_S = M_0$. In other cases the $A_\kappa = A_\lambda$ relation is relaxed [27], and/or κ is taken as a free parameter [29, 30], or the soft Higgs masses are allowed to deviate from M_0 [31] giving less constrained models. In the spirit of the CMSSM/mSuGra, we adhere to universality and use only λ to parametrize the singlet sector. This way, we keep all the attractive features of the CMSSM/mSuGra while the minimal extension alleviates problems rooted in the MSSM, making the NMSSM a more natural model.

As we have shown in our previous work [32], NmSuGra phenomenology bears a high similarity to the minimal supergravity motivated model. The most significant departures from a typical mSuGra model are the possibility of a singlino-dominated neutralino and the extended Higgs sector, which may provide new resonance annihilation channels and Higgs decay channels, potentially weakening the mass limit from LEP. The majority of NmSuGra phenomenology can be described in terms of the familiar mSuGra features [33]. The gross structure of the parameter space, for example, can be easily understood in terms of the predominant neutralino (co-)annihilation mechanisms. NmSuGra features the well known neutralino-slepton co-annihilation, Higgs resonance corridor annihilation and focus point regions, as well as small regions of mostly singlino-type neutralino annihilation via multiple channels. In the following discussions, we will rely on the similarity between our model and mSuGra to interpret the results of the likelihood scan, while paying special attention to all distinct phenomenological signatures.

3. Bayesian inference

Since several excellent papers have appeared on this subject recently [34, 35, 36, 37, 38], in this section, we summarize the concepts of Bayesian inference that we use in our analysis in a compact fashion. Our starting hypothesis H is the validity of the NmSuGra model. The conditional probability $\mathcal{P}(P|D;H)$ quantifies the validity of our hypothesis by giving the chance that the NmSuGra model reproduces the available experimental data D with its parameters set to values P. When this probability density is integrated over a region of the parameter space it yields the posterior probability that the parameter values fall into the given region.

Bayes' theorem provides us with a simple way to calculate the posterior probability distribution as

$$\mathcal{P}(P|D;H) = \mathcal{P}(D|P;H)\frac{\mathcal{P}(P|H)}{\mathcal{P}(D|H)}. \tag{3.1}$$

Here $\mathcal{P}(D|P;H)$ is the likelihood that the data is predicted by NmSuGra with a specified set of parameters. The a-priori distribution of the parameters within the theory $\mathcal{P}(P|H)$

is fixed by purely theoretical considerations independently from the data. The evidence $\mathcal{P}(D|H)$ gives the probability of the hypothesis in terms of the data alone. The latter can easily be seen from Bayes' theorem by multiplying both sides with $\mathcal{P}(D|H)$ and integrating for the full parameter space:

$$\mathcal{P}(D|H) = \int \mathcal{P}(D|P;H)\mathcal{P}(P|H)dP. \tag{3.2}$$

If the data under consideration are statistically independent, as in our case, the likelihood function factorizes

$$\mathcal{P}(D|P;H) = \prod_i \mathcal{L}_i(D,P;H), \tag{3.3}$$

where $\mathcal{L}_i$ is the likelihood associated with the ith measurable, and is given as a convolution

$$\mathcal{L}_i(D,P;H) = \mathcal{L}_i^E(D) \otimes \mathcal{L}_i^T(P;H). \tag{3.4}$$

If the experimental and theoretical likelihoods corresponding to the ith measurable, $\mathcal{L}_i^E$ and $\mathcal{L}_i^T$, are normally distributed, then the likelihood function is a Gaussian

$$\mathcal{L}_i(D,P;H) = \frac{1}{\sqrt{2\pi}\sigma_i}\exp(\chi_i^2(D,P;H)/2). \tag{3.5}$$

In this case the exponents

$$\chi_i^2(D,P;H)/2 = (d_i - t_i(P;H))^2/2\sigma_i^2, \tag{3.6}$$

are defined in terms of the experimental data $D = \{d_i \pm \sigma_{i,e}\}$ and theoretical predictions $T = \{t_i \pm \sigma_{i,t}\}$ for these measurables. Independent experimental and theoretical uncertainties combine into $\sigma_i^2 = \sigma_{i,e}^2 + \sigma_{i,t}^2$. In cases when the experimental data only specify a lower (or upper) limit, the corresponding likelihood function can be written in terms of the error function

$$\mathcal{L}_i(D|P;H) = \frac{1}{2}\mathrm{erfc}(\pm\sqrt{\chi_i^2(D,P;H)/2}). \tag{3.7}$$

Despite its dependence on several parameters, the likelihood function can easily be visualized by plotting profile likelihood distributions. These are constructed by finding the maximum likelihood hypersurface

$$\mathcal{L}^{max}(D|p_i;H) = \max_{p_1,\ldots,p_{i-1},p_{i+1},\ldots,p_n}(\mathcal{L}(D|P;H)). \tag{3.8}$$

and projecting this to one (or more functions) of the parameters. These profile likelihoods highlight the model regions where the likelihood is highest and lowest. Although this is certainly of interest, in the Bayesian context the estimated values of the parameters are determined by the posterior probability density.

While the posterior probability density $\mathcal{P}(P|D;H)$ depends on all the parameters $P = \{p_i\}$ of NmSuGra, it is useful to know the probability distribution of each single parameter p_i. This latter is referred to as the marginalized probability and given by

$$\mathcal{P}(p_i|D;H) = \int \mathcal{P}(P|D;H)dp_1...dp_{i-1}dp_{i+1}...dp_n. \tag{3.9}$$

Similarly to this, marginalization can be performed to two (or more) variables resulting in a two (or more) dimensional distribution:

$$\mathcal{P}(p_i, p_j|D;H) = \int \mathcal{P}(P|D;H) dp_1 ... dp_{i-1} dp_{i+1} ... dp_{j-1} dp_{j+1} ... dp_n. \tag{3.10}$$

Our main goal in this work is to evaluate marginalized probability distributions for the five theoretical parameters of the NmSuGra model.

Marginalization can also be performed to an arbitrary function (or several functions) of the parameters. The posterior probability density of an arbitrary function (of a subset) of the parameters $f(P)$ is obtained as

$$\mathcal{P}(f|D;H) = \int \delta(f - f(P)) \mathcal{P}(P|D;H) dP. \tag{3.11}$$

These marginalized probability distributions are useful when we compare various NmSuGra predictions to the experimental likelihood distributions to check the consistency of the model with the data, and when we assess the future detectability of the model.

It is also useful to introduce confidence level regions measured by relative probabilities. We define an x percent confidence level region $\mathcal{R}_x$ by the set of the minimal parameter regions supporting x percent of the total probability:

$$x = \left(\int_{\mathcal{R}_x} \mathcal{P} dP \right) \left(\int \mathcal{P} dP \right)^{-1}. \tag{3.12}$$

Here $\mathcal{P}$ can be a likelihood function or a posterior probability distribution, and the integral in the denominator extends to the full parameter space.

Profile likelihood distributions and posterior probability distributions carry different information about the theoretical parameter space. While the former expresses in which regions the model can or cannot fit the data, the latter gives the probability of the of a given parameter region in the light of the data. As Bayes theorem shows these two differ by the factors of the theoretical prior and the evidence. Setting the evidence aside as a trivial normalization factor, the prior should come from purely theoretical considerations, from an underlying theory perhaps. In the case of NmSuGra this information is highly uncertain and the a prior can be selected, at best, based on simplistic assumptions such as fine-tuning. For this reason in this work we resort to a trivial (uniform) prior, expressing the fact that we have no reliable theoretical information about the a-priori probability distribution over the parameter space.

Besides this difference marginalized posterior probabilities also capture information about the size and structure of the parameter space via the integration in Eq.s (3.9) and (3.10). In other words the volume of the parameter space, via the integration measure, affects the posterior probability. The likelihood profile do not contain this information. Thus, even with a prior uniform over the parameter space, this volume effect can substantially change the shape of posterior probability distributions compared to the profile likelihoods.

4. Likelihood analysis of NmSuGra

Our main intent is to calculate the posterior probability distributions for the five continuous parameters of NmSuGra and check the consistency of the model against available experimental data. To this end, we use the publicly available computer code NMSPEC [39] to calculate the spectrum of the superpartner masses and their physical couplings from the model parameters given in Eq. (2.12). Then, we use NMSSMTools 2.1.0 and micrOMEGAs 2.2 [40] to calculate the abundance of neutralinos (Ωh^2), the spin-independent neutralino-proton elastic scattering cross section (σ_{SI}), the NmSuGra contribution to the anomalous magnetic moment of the muon (Δa_μ), and various b-physics related quantities. All the experimental data D used in our likelihood analysis are listed in Table 1. Uncertainties arising in the supersymmetric calculation of Δa_μ and the b-physics related quantities are calculated using NMSSMTools. Among the standard input parameters, $m_b(m_b) = 4.214$ GeV and $m_t^{pole} = 171.4$ GeV are used.

As alluded to previously, the LEP mass limit for the standard model Higgs $m_h > 114.4$ GeV is not applicable to the lightest scalar in the NMSSM. Specifically, any component of the gauge-singlet scalar in the lightest Higgs would decrease its couplings to gauge bosons. We calculate the modified limit according to Ref. [41], by comparing the NMSSM coupling of the lightest scalar to the Z boson with that of the standard model. Furthermore, in the NMSSM there is the possibility of a light pseudoscalar field a with $m_a < m_W$ to which the lightest Higgs could decay as $h \to aa$ without subsequent charged decays. For these rare occurances the LEP Higgs limit is further relaxed.

Using the above specified tools, we generate theoretical predictions for NmSuGra in the following part of its parameter space:

$$\begin{aligned} 0 < M_0 < 5 \text{ TeV}, \quad 0 < M_{1/2} < 2 \text{ TeV}, \quad -3 \text{ TeV} < A_0 < 5 \text{ TeV}, \\ 0 < \tan\beta < 60, \quad 10^{-5} < \lambda < 0.6, \quad \text{sign}(\mu) > 0. \end{aligned} \tag{4.1}$$

In this work, we only consider the positive sign of μ because, similarly to mSuGra [34], the likelihood function is suppressed by Δa_μ and $B(b \to s\gamma)$ in the negative μ region. When calculating posterior probabilities, we use a uniform prior; or equivalently, we define the measure of the integration in Eq.s (3.9) and (3.10) by weighting all parts of the parameter space equally. We evaluate the integrals over the likelihood function in two different ways. In the first method, we simply select random model points from the parameter space according to a uniform distribution. In the second, we adopt the Markov Chain Monte Carlo technique as described in [51]. The Markov Chain implements the Metropolis algorithm, and is more efficient than the random scan in terms of the proportion of viable points scanned. However, by construction the Markov Chain has a tendency to focus strongly on high-likelihood regions and so the results of individual chains can be somewhat sporadic. As the five dimensional NmSuGra parameter space is not prohibitively large, the uniform random scan gives a good means of checking the Markov Chain as it provides very consistent results over different runs, although with somewhat less fine detail in the likelihood distribution. In general, for all of our results the two different methods are in good agreement.

4.1 Profile likelihoods

Turning to our numerical results, in Figure 1 we show profile likelihood distributions projected to individual input parameters. In these plots, for ease of interpretation, we normalize the profile likelihoods such that a model point fitting perfectly the data (with $\chi^2 = 0$) would result in a likelihood value of 1.

These likelihood profiles tell us the best fit of NmSuGra predictions to experimental and where in the parameter space they occur. Regions of high likelihood are not difficult to find within NmSuGra. For our results, the model point with the highest likelihood has a $\chi^2_{total} = 1.85$ and there exist ample parameter regions with the most likely $\chi^2/d.o.f \approx 1$.

The top left frame of Figure 1 indicates that the highest likelihood regions lie at low values of the common scalar mass M_0, within $0 < M_0 \leq 0.5$ TeV ($0 < M_0 \leq 1.5$ TeV) at 68 (95) % confidence level. This happens because, with the exception of some of the b-physics observables, the experimental data mostly favor the sfermion-neutralino co-annihilation region, lying around low M_0 values. Higgs resonance corridors at intermediate M_0 still give a reasonable fit, while the likelihood function tends to drop in the focus point region at high M_0 values due mainly to Δa_μ disfavoring high sparticle masses (consistent with our earlier results [32]).

Although the highest likelihood is about 3.5×10^{-3} at $M_0 = 5$ TeV, this corresponds

Observable	Limit type	$d_i \pm \sigma_{i,e}$	$\sigma_{i,t}^{SUSY}$
m_h	lower limit	up to 114.4 GeV [41]	3.0 GeV [42]
$m_{\tilde{\tau}_1}$	lower limit	73.0 or[1] 87.0 GeV [38]	10 %
$m_{\tilde{e}_R}$	lower limit	73.0 or[1] 100. GeV [38]	10 %
$m_{\tilde{\mu}_R}$	lower limit	73.0 or[1] 95.0 GeV [38]	10 %
$m_{\tilde{\nu}_e}$	lower limit	43.0 or[1] 94.0 GeV [38]	10 %
$m_{\tilde{t}_1}$	lower limit	65.0 or[1] 95.0 GeV [38]	10 %
$m_{\tilde{b}_1}$	lower limit	59.0 or[1] 95.0 GeV [38]	10 %
$m_{\tilde{q}_1}$	lower limit	318.0 GeV [38]	10 %
$m_{\tilde{W}_1}$	lower limit	43.0 or[2] 92.4 GeV [38]	10 %
$m_{\tilde{Z}_1}$	lower limit	50.0 GeV [38]	10 %
$m_{\tilde{g}}$	lower limit	195.0 GeV [38]	10 %
Δa_μ	central value	$(29.0 \pm 9.0) \times 10^{-10}$ [43]	negligible
Δm_d	central value	$(5.07 \pm 0.04) \times 10^{11}$ ps^{-1} [44]	1 % [40]
$B(b \to s\gamma)$	central value	$(3.50 \pm 0.17) \times 10^{-4}$ [44]	10 % [45]
$B(B^+ \to \tau + \nu_\tau)$	central value	$(1.73 \pm 0.35) \times 10^{-4}$ [46]	10 % [40]
$B(B_s \to \mu^+\mu^-)$	upper limit	4.7×10^{-8} [46]	10 % [47]
Ωh^2	upper limit	0.1143 ± 0.0034 [48]	10 % [40]
σ_{SI}	upper limit	CDMS 2008 [49]	20 % [50]

Table 1: Observables used in the calculation of the posterior probability distribution $\mathcal{P}(P|D;H)$. Experimental data are listed under column $d_i \pm \sigma_{i,e}$, and typical uncertainties related to the NmSuGra calculations are under $\sigma_{i,t}^{SUSY}$.

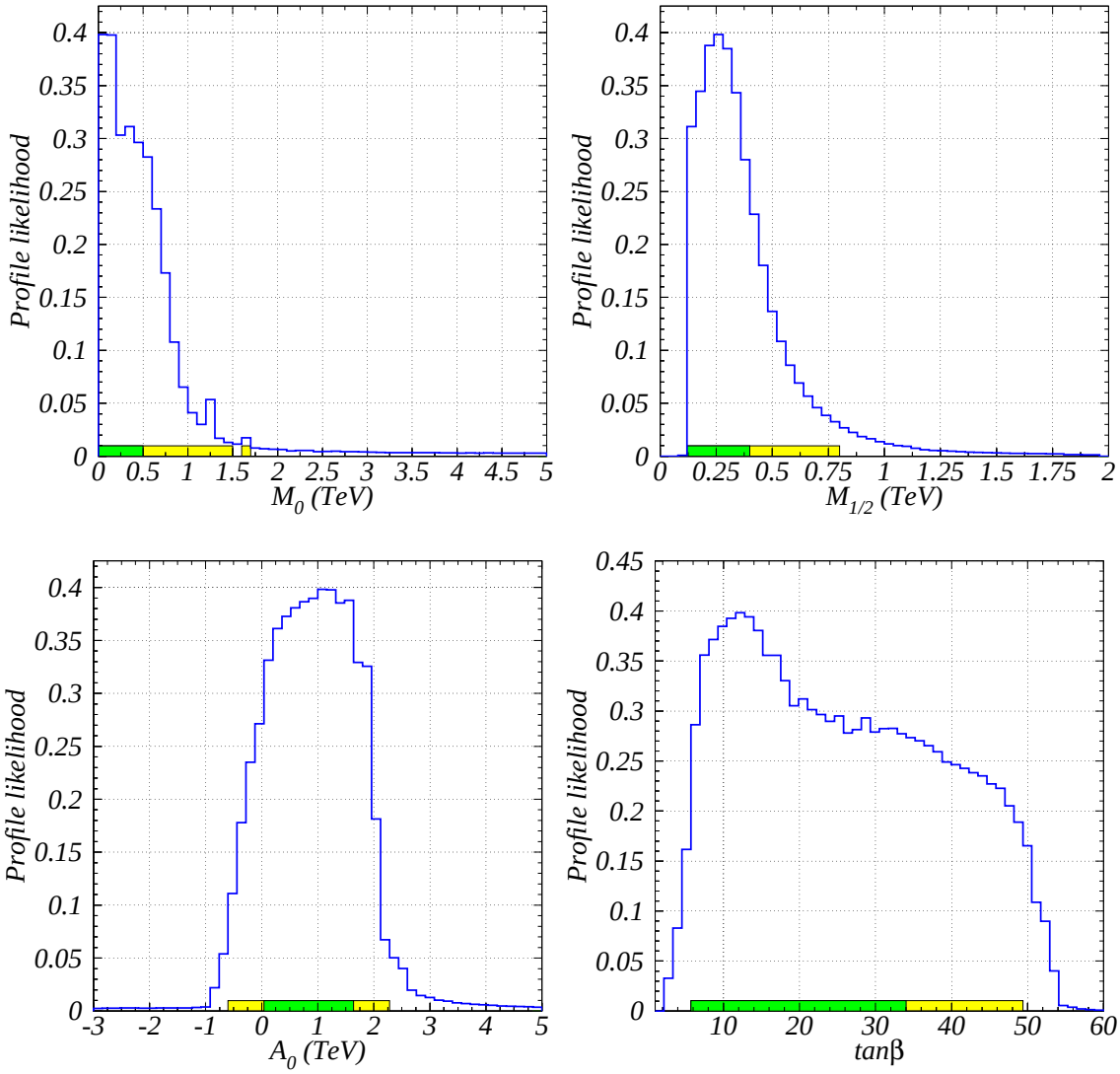

Figure 1: Profile likelihood distributions of the NmSuGra input parameters. Green (yellow) coloring indicates 68 (95) percent confidence level regions.

to a combined $\chi^2_{total} < 12$. Discarding direct (s)particle mass limits (which don't affect the focus point) and counting only the last seven entries in Table 1, this corresponds to $\chi^2/d.o.f < 2$ in average, which is not a bad fit. This means that viable model points remain in the focus point, although with less likelihood than those at lower M_0 values.

We can draw a similar conclusion for the common gaugino mass $M_{1/2}$ from the next frame of Figure 1. The data appear to prefer small to moderate values of $M_{1/2}$ for NmSuGra falling in the region $0.18 \leq M_{1/2} \lesssim 0.35$ TeV ($0.18 \leq M_{1/2} \lesssim 0.8$ TeV) with a 68 (95) % confidence level. The likelihood is suppressed at high $M_{1/2}$ by Δa_μ.

The same is evident from the profile likelihood of the common tri-linear parameter A_0,

which has two maximal regions, one slightly negative but close to zero and another around 1 TeV. The data show a high preference toward $\tan\beta \sim 5$ and somewhat lower toward the $5 \lesssim \tan\beta \lesssim 35$ region. The Higgs-singlet-Higgs coupling λ (not shown) has a rather featureless likelihood profile tapering down above $\lambda > 0.5$ at a 95 % confidence level.

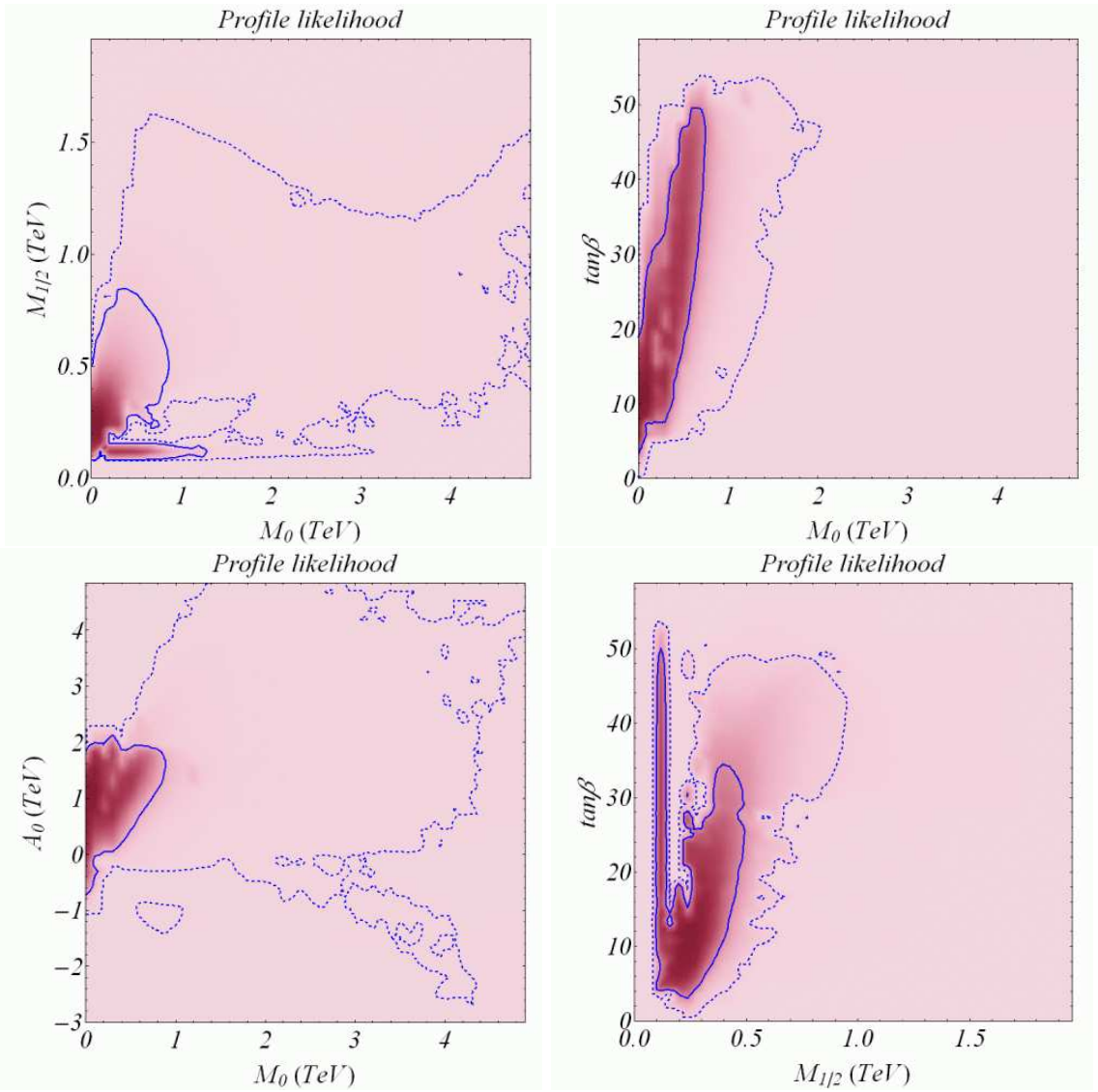

Figure 2: Profile likelihood distributions as the function of pairs of NmSuGra input parameters. The higher likelihood regions are darker. Solid (dotted) blue lines indicate 68 (95) percent confidence level contours.

In Figure 2 we show profile likelihood distributions as the function of various pairs of NmSuGra input parameters. Solid (dotted) blue lines indicate 68 (95) percent confidence level contours. According to the first frame the highest likelihoods coincide with the stau-neutralino and the adjoint (pseudoscalar and heavier) Higgs resonance region. Annihilation via the lightest Higgs in the s-channel is also prominent. The last frame supports this giving

us the insight that stau-neutralino co-annihilation is dominant at low to moderate $\tan\beta$, while resonant annihilation via the lightest Higgs boson is essentially independent of $\tan\beta$.

The first three frames clearly indicate that the likelihood in the focus point, for high M_0, is suppressed by the anomalous magnetic moment of the muon, as we found earlier. The relatively featureless second frame is included for reference and completness; later we will use the posterior probability conterpart of this distribution to confirm the location of the focus point at high $\tan\beta$. Although the asymmetry is moderate, most of the high likelihood region has positive A_0 as can be read from the second frame.

4.2 Posterior probabilities

While the likelihood function may peak in certain regions of the parameter space, signaling that the theory predictions fit well the experiment, this alone does not give information on the probability of various parameter regions. It may happen, for example, that the theory has high (moderate) likelihood over a small (large) parameter region. According to Bayes theorem the probability assigned to a parameter region is the accumulated likelihood over the given region of parameter space.

Furthermore, if a theory has many parameters, or more generally a large parameter space, then one could expect a better fit to experiment would be possible compared to the case with a fewer theoretical parameters. However such a model is arguably less natural (or possibly more contrived). A marginalized posterior probability depends on the size of the parameter space and the cumulative magnitude of the likelihood function over this space, rather than simply peak values. As a consequence, larger parameter spaces with low likelihoods incur an inherent penalty to the posterior probability as unitarity suppresses the posterior probability, in accordance with Occam's principle.

We show the posterior probability marginalized to the five input parameters in Figure 3. Since the integral of the posterior probability distribution marginalized to a given parameter p_i

$$\mathcal{P}(a < p_i < b|D;H) = \int_a^b \mathcal{P}(p_i|D;H)dp_i, \tag{4.2}$$

yields the probability that p_i falls in the interval $[a,b]$, we normalize the marginalized posterior densities such that the area under the distribution is unity.

The top left frame of Figure 3 shows the posterior probability marginalized to M_0. As expected, based on the profile likelihood for M_0, the posterior peaks at low M_0 values. But notably, it peaks at a higher value, around $M_0 \simeq 0.5$ TeV, than the likelihood function. This difference is a good example of the volume effect: the sfermion-neutralino co-annihilation region requires a high fine-tuning between the sfermion (typically stau) and neutralino masses, and consequently it is extremely narrow in M_0. Since it covers such a small region its posterior probability is suppressed even though its likelihood is high.

The exact opposite happens in the focus point region at high M_0. The prominent rise of the posterior probability toward high M_0 values clearly comes from the overwhelming size of the focus point region. Most of this enhancement happens at high $\tan\beta(\sim 50)$ where

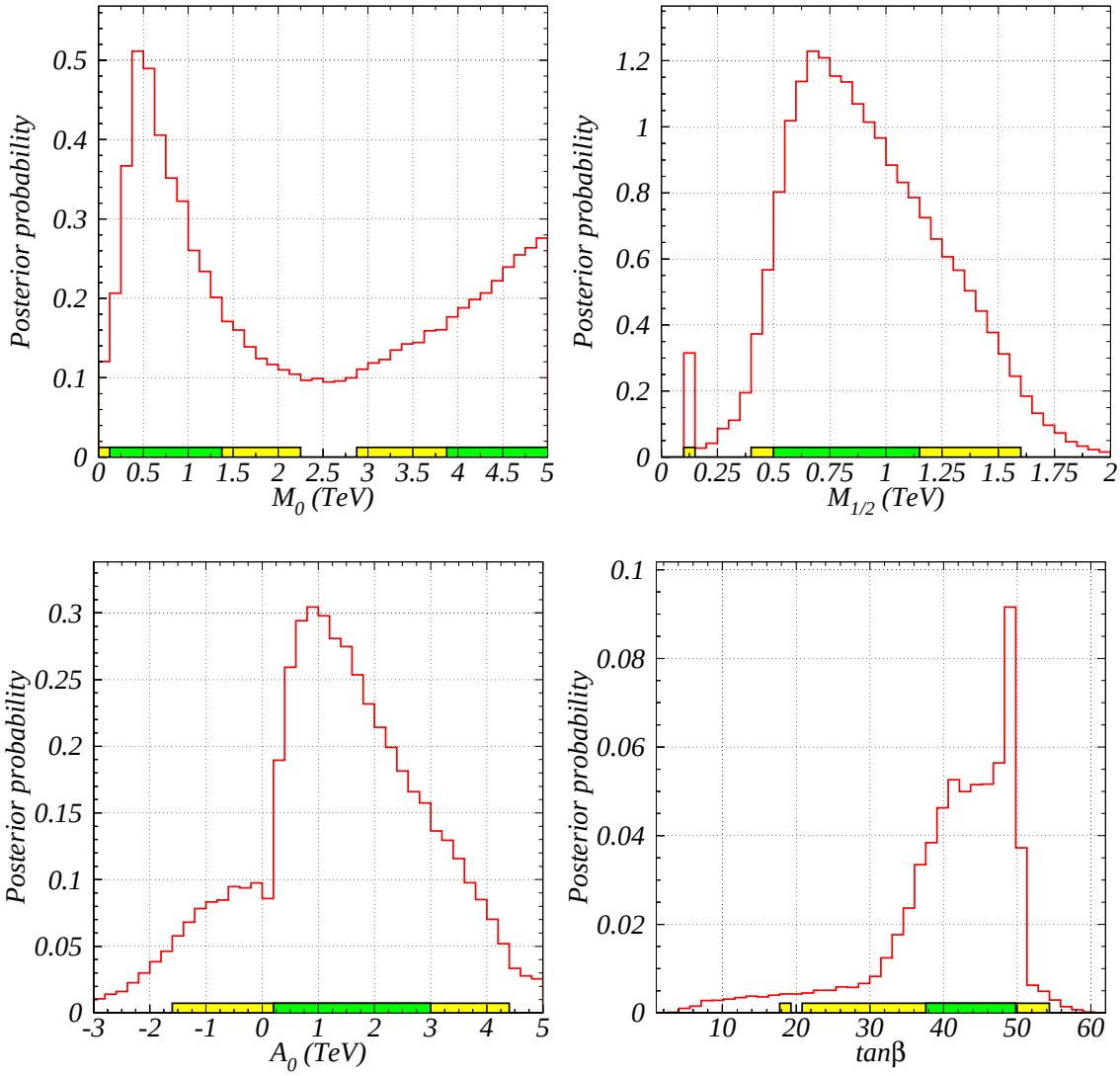

Figure 3: Posterior probability densities marginalized to the NmSuGra input parameters.

the traditional focus point region merges with multiple Higgs resonance corridors creating very wide regions consistent with WMAP.

The posterior probability distribution of $M_{1/2}$, in the top right frame of Figure 3, develops two maxima. A narrow peak is close to 150 GeV, and a wide one around 700 GeV. In the dark matter context, the former corresponds to neutralinos resonantly self-annihilating via the lightest scalar Higgs boson in the s-channel. This 'sweet spot' emerges as a combined high-likelihood and volume effect, as we will see a bit later. Most of the wide peak comes from neutralinos resonance annihilating via the heavier scalar and pseudo-scalar Higgses. These regions tend to create wide Higgs channels consistent with WMAP.

The same volume effect boosts the moderately positive A_0 region of the likelihood

function in the posterior probability shown in the lower left frame of Figure 3. An even more prominent volume enhancement reshapes the posterior probability around $\tan\beta \sim 40-50$, as shown in the lower right frame. The wide bump originates from Higgs resonance corridors, while the narrow peak from the focus point region which also raises the posterior at high M_0.

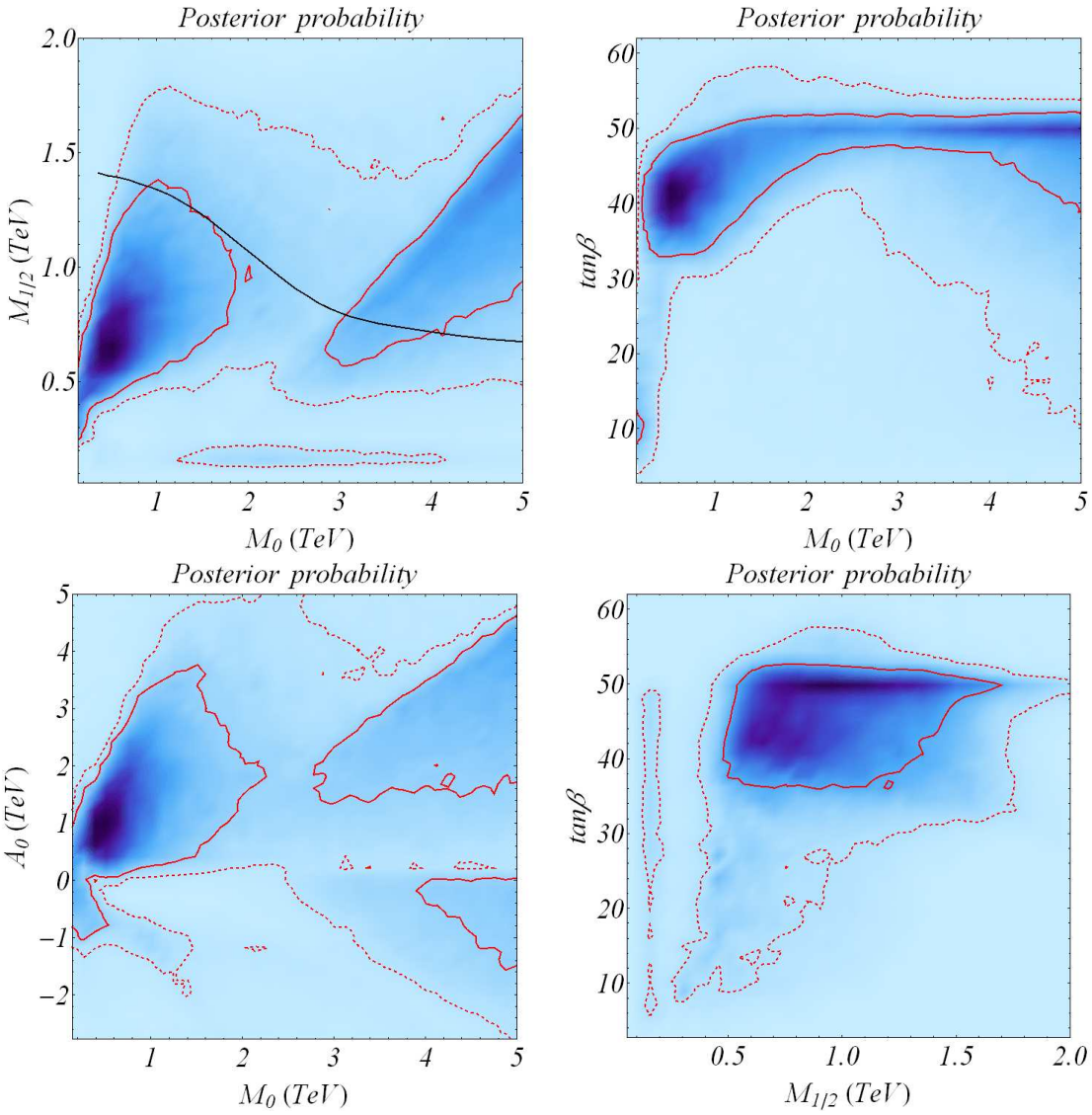

Figure 4: Posterior probability densities marginalized to pairs of NmSuGra input parameters. The higher probability regions are darker. Solid (dotted) red lines indicate 68 (95) percent confidence level contours. On the top left frame the diagonal black curve shows the estimated reach of the LHC for 100 fb^{-1} luminosity [52].

The effects described are evident from the posterior probability distributions marginalized to different pairs of NmSuGra input parameters, as Figure 4 shows. In the top left frame we show the posterior probability marginalized to the plane of the common scalar

and gaugino masses, M_0 vs. $M_{1/2}$. The slepton co-annihilation region combined with Higgs resonance corridors, at low M_0 and low to moderate $M_{1/2}$ supports most of the probability. This region is clearly separated from the focus point at high M_0 and moderate to high $M_{1/2}$, large part of which falls in the 68 % confidence level.

At the lowest $M_{1/2}$ values lies a Higgs annihilation strip, where the lightest neutralinos resonance annihilate via the lightest scalar Higgs boson. Part of this region is allowed in NmSuGra due to the somewhat relaxed mass limit by LEP on the lightest Higgs. The narrowness of this strip correlates with the smallness of the lightest Higgs width. In this region the likelihood can be high, and when integrating over M_0 volume is accumulated. This explains the narrow, isolated peak at the lowest values in the posterior probability marginalized to $M_{1/2}$.

The top right frame of Figure 4 shows the distribution of the posterior probability in the M_0 vs. $\tan\beta$ frame. This makes it clear that most of the probable points are carried by Higgs resonant corridors toward higher $\tan\beta$, and the sfermion co-annihilation, due to its narrowness in M_0, falls only in the 95 % confidence, but is outside the 68 % region. The exception is a minute corner of the parameter space at very low M_0, $M_{1/2}$, and $\tan\beta \sim 10$ where all theoretical results conspire to match experiment, raising the sfermion co-annihilation region into the 68 % confidence region. At the opposite, high M_0 and $\tan\beta$ corner multiple Higgs resonances combined with neutralino-chargino co-annihilation in the focus point lead to substantial contribution to the total probability.

The lower left frame of Figure 4 shows that positive values of A_0 are preferred over negative ones, because Higgs resonance annihilation occurs overwhelmingly at low to moderately positive values of A_0. The focus point, containing less probability, extends further along both positive and negative A_0. The lower right frame confirms that resonance annihilation via the lightest Higgs boson happens at all $\tan\beta$ values. As previously mentioned, the resonance annihilation via heavier Higgs bosons and the focus point is only dominant at high $\tan\beta$.

5. Experimental detection of NmSuGra

Figure 1, in itself, is encouraging for the prospects of discovery of NmSuGra at the LHC. We can quantify this statement more precisely by constructing the profile likelihoods for the lightest superpartners and the gluino. Figure 5 shows that in the most likely NmSuGra model regions the mass of the lightest neutralino falls in the $50 \leq m_{\tilde{Z}_1} \lesssim 200$ (375) GeV region at 68 (95) % confidence level. In these regions the lighter stau is relatively light, while the gluino and the lighter stop are moderately heavy.

The likelihood function of the lightest stop features a narrow peak at the lowest masses. This tells us that high likelihoods are possible to achieve in NmSuGra parameter regions where the lightest stop co-annihilates with a neutralino, with both sparticle masses around 100 GeV. This region, featuring low M_0, $M_{1/2}$, $\tan\beta$ and moderate A_0, is very interesting phenomenologically, since at these parameter values electroweak baryogenesis can solve the baryon asymmetry problem in the MSSM and in its singlet extensions [53, 54, 55, 56]. This region is excluded in mSuGra by the LEP Higgs mass limit, but in NmSuGra this limit is

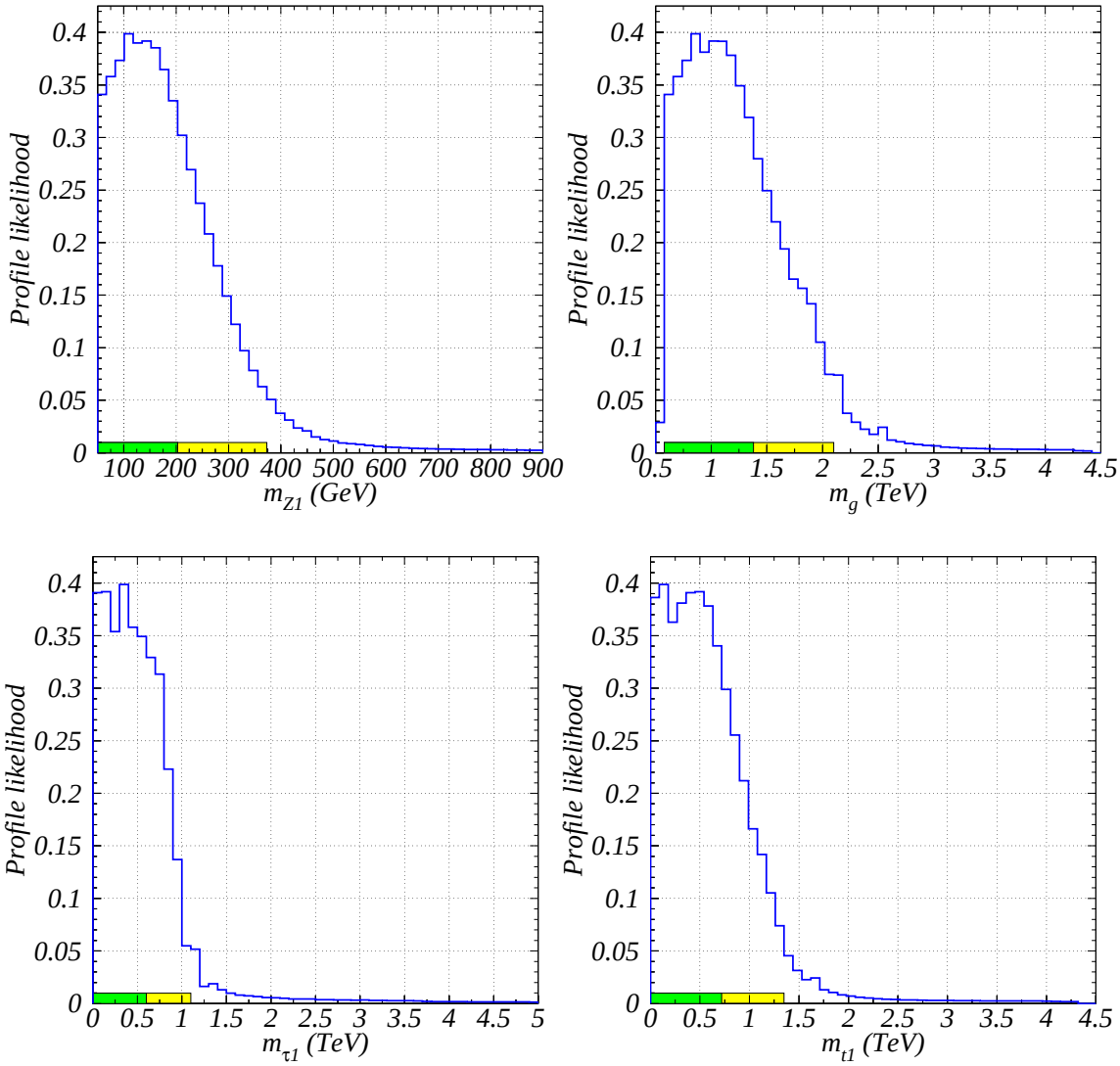

Figure 5: Profile likelihood distributions of various sparticle masses. Green (yellow) coloring indicates 68 (95) percent confidence level regions.

relaxed. Thus, in the NmSuGra model a strongly first order electroweak phase transition might be made possible by a light stop, a moderate size singlet-Higgs coupling λ, or the combination of these.

After integrating the likelihood function over the considered NmSuGra parameter space, we can assess the detection prospects at the LHC. The posterior probability in the top left frame of Figure 6 indicates that the lightest neutralino mass is expected to lie in the $175(125) \leq m_{\tilde{Z}_1} \lesssim 475(675)$ GeV region at 68 (95) % confidence level. The 95 % confidence level region also includes a small window around 70 GeV. The shift toward heavier masses, relative to the likelihood functions, occurred due to heavier average sparticle

masses in the focus point.

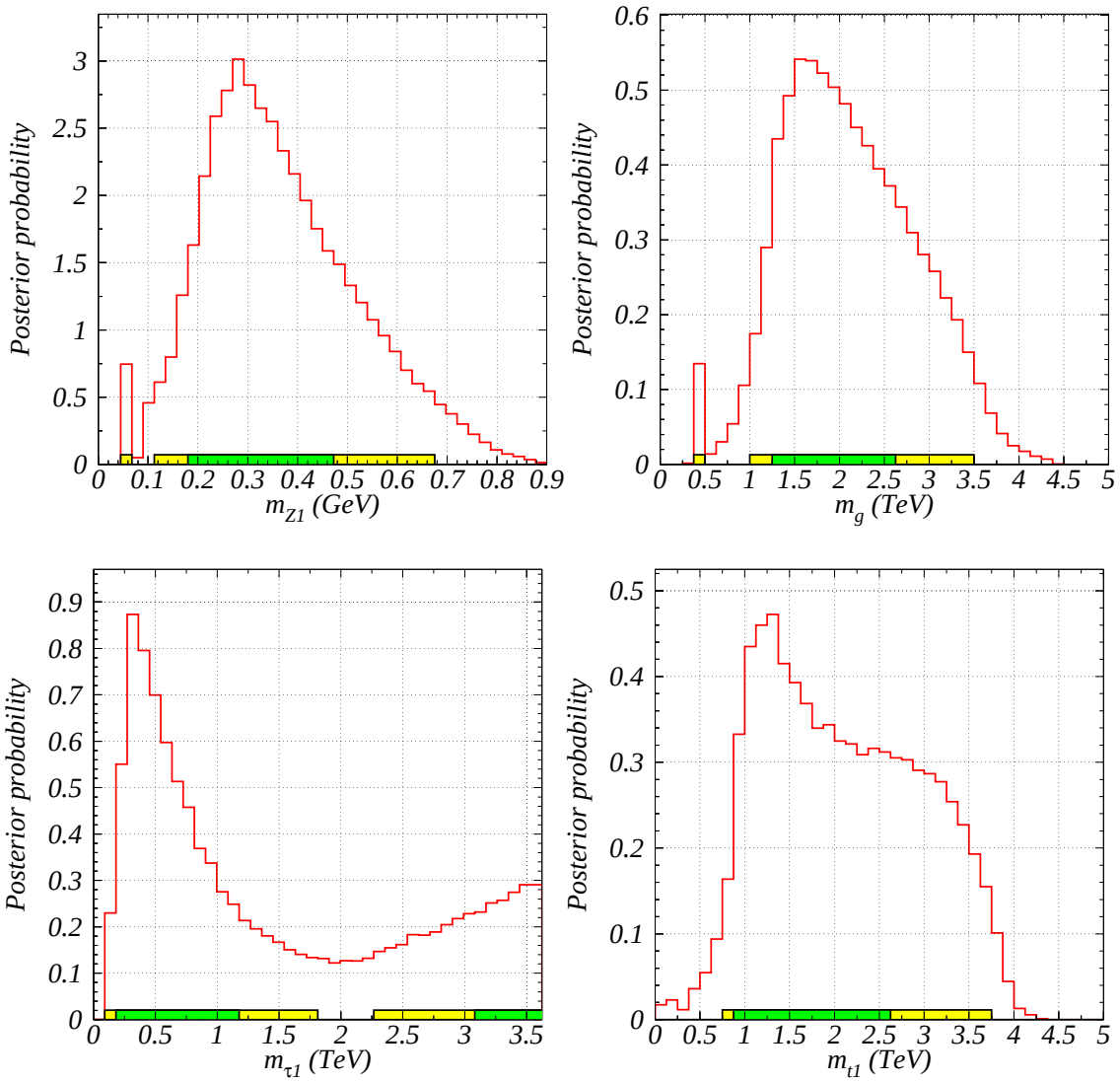

Figure 6: Posterior probability densities marginalized to various sparticle masses.

Unfortunately, this effect moves part of the NmSuGra parameter space out of the reach of the LHC, as shown by the posterior probability distribution of the gluino mass. In the mSuGra model the LHC is able to reach about 3 TeV gluinos with 100 fb^{-1} luminosity, provided the model has low M_0 [52]. In the focus point this reach is reduced to about 1.75 TeV. This means, just as in mSuGra, that part of the viable parameter space will remain out of reach of the LHC.

This conclusion is quantified even better by the estimated LHC reach displayed in the top left frame of Figure 3. From there it is evident that with 100 fb^{-1} the LHC will be able to cover sfermion co-annihilations and Higgs resonances that fall into the 68 % confidence

region, together with a small part of the focus point. But the LHC will stop short of fully exploring the Higgs resonances and the focus point at high $M_{1/2}$.

In the lower left frame of Figure 6 the posterior probability distribution of the lightest stau mass mirrors that of M_0. The next frame shows that the lighter stop is also expected to be heavier than the likelihood function alone suggests. Even the sharp peak at low values in the stop likelihood function is overwhelmed due to the minute volume of the parameter space it occupies.

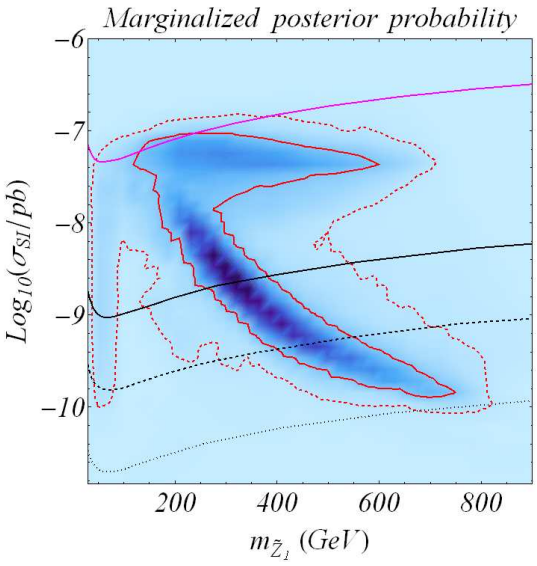

Figure 7: Posterior probability density marginalized to the spin-independent neutralino-nucleon elastic recoil cross section and the lightest neutralino mass. Confidence level contours are shown for 68 (solid red) and 95 (dashed red) %. The present (solid magenta) and projected reach of the upgraded CDMS experiment is shown for a 25 (solid black), 100 (dashed black), and a 1000 (dotted black) kg detector.

While the LHC will not be able to cover the full viable NmSuGra parameter space, fortunately measurements in the near future will explore a large part of the remaining region. Amongst the most promising experiments complementing the capabilities of the LHC are the measurements of the spin-independent neutralino-nucleon elastic recoil cross section, σ_{SI}. From several of these experiments, we single out CDMS as the most illustrative example. Figure 7 shows the posterior probability density marginalized to the plane of σ_{SI} and the lightest neutralino mass.

The magenta line toward the top of the plot is the present upper limit set by CDMS in 2008 [49]. Although this limit is included in our likelihood function, due to our generous estimate of the theoretical error (20%), the combined theoretical-experimental likelihood function still allows a small region above the experimental exclusion. The black line between $10^{-9} < \sigma_{SI} < 10^{-8}$ shows the estimated reach of a 25 kg super-CDMS. The lower dashed and dotted black lines show the estimated CDMS reach for a 100 and 1000 kg detector [57].

This plot clearly shows that direct detection experiments, if performs as expected, can play a pivotal role in discovering or ruling out simple constrained supersymmetric scenarios. It is interesting to observe that a one ton version of CDMS alone would be able to cover the full relevant NmSuGra parameter space. But the most important message is that even a 25 kg CDMS will reach a substantial part of the focus point region, complementing the LHC.

In the posession of the above results, we can quantify the chances for the discovery of NmSuGra at the LHC by calculating the ratio of posterior probabilities with and without

the LHC reach:

$$\frac{\int_{\text{within LHC reach}} \mathcal{P}(p_i|D;H)dp_i}{\int_{\text{outside LHC reach}} \mathcal{P}(p_i|D;H)dp_i} = 0.57. \tag{5.1}$$

According to this the odds of finding NmSuGra at the LHC are 4:3 (assuming, of course, that the model is chosen by Nature). We can also easily calculate the probability of the discovery of NmSuGra at the LHC combined with a ton equivalent of CDMS (CDMS1T):

$$\frac{\int_{\text{within LHC+CDMS1T reach}} \mathcal{P}(p_i|D;H)dp_i}{\int_{\text{outside LHC+CDMS1T reach}} \mathcal{P}(p_i|D;H)dp_i} = 0.99. \tag{5.2}$$

This means that according to the present data the NmSuGra model lies within the combined reach of the LHC and CDMS1T at 99 percent confidence level. The two experiments combined are essentially guaranteed to discover this model! This result strongly underlines the complementarity of collider and direct dark matter searches.

6. Conclusions

The next-to-minimal supergravity motivated model is one of the more compelling models for physics beyond the standard model due to its naturalness and simplicity. In this work we applied a thorough statistical analysis to NmSuGra based on numerical comparisons with present experimental data. Using Bayesian inference we found that significant regions of the NmSuGra parameter space remain viable under current constraints, and that the LHC has a 57 % chance to discover these regions. Furthermore, we found that the predicted LHC reach combined with the projected sensitivity of a ton equivalent of CDMS covers the viable NmSuGra parameter region at 99 % confidence level. This result underlines the complementarity of the LHC and direct dark matter searches in discovering new physics at the TeV scale.

Since much of the NmSuGra phenomenology appears to be very similar to that of the MSSM after imposing minimal supergravity (mSuGra or CMSSM), we expect these conclusions to be broadly valid within the constrained MSSM as well. While this is good news from the theoretical viewpoint, it poses a challenge to the LHC experimentalists to disentangle these models.

7. Acknowledgments

The authors are indebted to D. Kahawala, F. Wang, L. Roszkowski, and M. White for invaluable discussions on various aspects of the NMSSM and the likelihood analysis. This research was funded in part by the Australian Research Council under Project ID DP0877916.

References

[1] J. E. Kim and H. P. Nilles, *The mu Problem and the Strong CP Problem*, *Phys. Lett.* **B138** (1984) 150.

[2] G. F. Giudice, *Naturally Speaking: The Naturalness Criterion and Physics at the LHC*, *In Kane, Gordon (ed.), Pierce, Aaron (ed.): Perspectives on LHC physics, 155-178* (2008) [arXiv:0801.2562].

[3] R. Dermisek and J. F. Gunion, *Escaping the large fine tuning and little hierarchy problems in the next to minimal supersymmetric model and h –¿ a a decays*, *Phys. Rev. Lett.* **95** (2005) 041801, [hep-ph/0502105].

[4] M. Bastero-Gil, C. Hugonie, S. F. King, D. P. Roy, and S. Vempati, *Does LEP prefer the NMSSM?*, *Phys. Lett.* **B489** (2000) 359–366, [hep-ph/0006198].

[5] J. F. Gunion, *New (and Old) Perspectives on Higgs Physics*, *AIP Conf. Proc.* **1030** (2008) 94–103, [arXiv:0804.4460].

[6] P. Fayet, *Supergauge Invariant Extension of the Higgs Mechanism and a Model for the electron and Its Neutrino*, *Nucl. Phys.* **B90** (1975) 104–124.

[7] H. P. Nilles, M. Srednicki, and D. Wyler, *Weak Interaction Breakdown Induced by Supergravity*, *Phys. Lett.* **B120** (1983) 346.

[8] J. M. Frere, D. R. T. Jones, and S. Raby, *Fermion Masses and Induction of the Weak Scale by Supergravity*, *Nucl. Phys.* **B222** (1983) 11.

[9] J. P. Derendinger and C. A. Savoy, *Quantum Effects and SU(2) x U(1) Breaking in Supergravity Gauge Theories*, *Nucl. Phys.* **B237** (1984) 307.

[10] B. R. Greene and P. J. Miron, *SUPERSYMMETRIC COSMOLOGY WITH A GAUGE SINGLET*, *Phys. Lett.* **B168** (1986) 226.

[11] J. R. Ellis *et. al.*, *PROBLEMS FOR (2,0) COMPACTIFICATIONS*, *Phys. Lett.* **B176** (1986) 403.

[12] L. Durand and J. L. Lopez, *Upper Bounds on Higgs and Top Quark Masses in the Flipped SU(5) x U(1) Superstring Model*, *Phys. Lett.* **B217** (1989) 463.

[13] M. Drees, *Supersymmetric Models with Extended Higgs Sector*, *Int. J. Mod. Phys.* **A4** (1989) 3635.

[14] J. R. Ellis, J. F. Gunion, H. E. Haber, L. Roszkowski, and F. Zwirner, *Higgs Bosons in a Nonminimal Supersymmetric Model*, *Phys. Rev.* **D39** (1989) 844.

[15] P. N. Pandita, *Radiative corrections to the scalar Higgs masses in a nonminimal supersymmetric Standard Model*, *Z. Phys.* **C59** (1993) 575–584.

[16] P. N. Pandita, *One loop radiative corrections to the lightest Higgs scalar mass in nonminimal supersymmetric Standard Model*, *Phys. Lett.* **B318** (1993) 338–346.

[17] U. Ellwanger, M. Rausch de Traubenberg, and C. A. Savoy, *Particle spectrum in supersymmetric models with a gauge singlet*, *Phys. Lett.* **B315** (1993) 331–337, [hep-ph/9307322].

[18] B. Ananthanarayan and P. N. Pandita, *Particle Spectrum in the Non-Minimal Supersymmetric Standard Model with* $\tan\beta \simeq m_t/m_b$, *Phys. Lett.* **B371** (1996) 245–251, [hep-ph/9511415].

[19] B. Ananthanarayan and P. N. Pandita, *The nonminimal supersymmetric standard model with tan Beta approximately = m(t) / m(b)*, *Phys. Lett.* **B353** (1995) 70–78, [hep-ph/9503323].

[20] B. Ananthanarayan and P. N. Pandita, *The Non-Minimal Supersymmetric Standard Model at Large* $\tan\beta$, *Int. J. Mod. Phys.* **A12** (1997) 2321–2342, [hep-ph/9601372].

[21] U. Ellwanger, M. Rausch de Traubenberg, and C. A. Savoy, *Phenomenology of supersymmetric models with a singlet*, *Nucl. Phys.* **B492** (1997) 21–50, [hep-ph/9611251].

[22] T. Elliott, S. F. King, and P. L. White, *Unification constraints in the next-to-minimal supersymmetric standard model*, *Phys. Lett.* **B351** (1995) 213–219, [hep-ph/9406303].

[23] S. F. King and P. L. White, *Resolving the constrained minimal and next-to-minimal supersymmetric standard models*, *Phys. Rev.* **D52** (1995) 4183–4216, [hep-ph/9505326].

[24] U. Ellwanger and C. Hugonie, *NMHDECAY 2.0: An Updated program for sparticle masses, Higgs masses, couplings and decay widths in the NMSSM*, *Comput. Phys. Commun.* **175** (2006) 290–303, [hep-ph/0508022].

[25] C. Panagiotakopoulos and K. Tamvakis, *Stabilized NMSSM without domain walls*, *Phys. Lett.* **B446** (1999) 224–227, [hep-ph/9809475].

[26] C. Panagiotakopoulos and A. Pilaftsis, *Higgs scalars in the minimal non-minimal supersymmetric standard model*, *Phys. Rev.* **D63** (2001) 055003, [hep-ph/0008268].

[27] C. Hugonie, G. Belanger, and A. Pukhov, *Dark Matter in the Constrained NMSSM*, *JCAP* **0711** (2007) 009, [arXiv:0707.0628].

[28] A. Djouadi, U. Ellwanger, and A. M. Teixeira, *The constrained next-to-minimal supersymmetric standard model*, *Phys. Rev. Lett.* **101** (2008) 101802, [arXiv:0803.0253].

[29] G. Belanger, F. Boudjema, C. Hugonie, A. Pukhov, and A. Semenov, *Relic density of dark matter in the NMSSM*, *JCAP* **0509** (2005) 001, [hep-ph/0505142].

[30] D. G. Cerdeno, E. Gabrielli, D. E. Lopez-Fogliani, C. Munoz, and A. M. Teixeira, *Phenomenological viability of neutralino dark matter in the NMSSM*, *JCAP* **0706** (2007) 008, [hep-ph/0701271].

[31] A. Djouadi *et. al.*, *Benchmark scenarios for the NMSSM*, *JHEP* **07** (2008) 002, [arXiv:0801.4321].

[32] C. Balazs and D. Carter, *Discovery potential of the next-to-minimal supergravity motivated model*, arXiv:0808.0770.

[33] H. Baer and C. Balazs, *Chi**2 analysis of the minimal supergravity model including WMAP, g(mu)-2 and b –¿ s gamma constraints*, *JCAP* **0305** (2003) 006, [hep-ph/0303114].

[34] F. Feroz *et. al.*, *Bayesian Selection of sign(mu) within mSUGRA in Global Fits Including WMAP5 Results*, *JHEP* **10** (2008) 064, [arXiv:0807.4512].

[35] R. Trotta, F. Feroz, M. P. Hobson, L. Roszkowski, and R. Ruiz de Austri, *The Impact of priors and observables on parameter inferences in the Constrained MSSM*, *JHEP* **12** (2008) 024, [arXiv:0809.3792].

[36] M. E. Cabrera, J. A. Casas, and R. Ruiz de Austri, *Bayesian approach and Naturalness in MSSM analyses for the LHC*, *JHEP* **03** (2009) 075, [arXiv:0812.0536].

[37] F. Feroz, M. P. Hobson, L. Roszkowski, R. Ruiz de Austri, and R. Trotta, *Are BR(b-¿s gamma) and (g-2)_muon consistent within the Constrained MSSM?*, arXiv:0903.2487.

[38] S. S. AbdusSalam, B. C. Allanach, F. Quevedo, F. Feroz, and M. Hobson, *Fitting the Phenomenological MSSM*, arXiv:0904.2548.

[39] U. Ellwanger and C. Hugonie, *NMSPEC: A Fortran code for the sparticle and Higgs masses in the NMSSM with GUT scale boundary conditions*, *Comput. Phys. Commun.* **177** (2007) 399–407, [hep-ph/0612134].

[40] G. Belanger, F. Boudjema, A. Pukhov, and A. Semenov, *micrOMEGAs2.0: A program to calculate the relic density of dark matter in a generic model*, *Comput. Phys. Commun.* **176** (2007) 367–382, [hep-ph/0607059].

[41] V. Barger, P. Langacker, H.-S. Lee, and G. Shaughnessy, *Higgs sector in extensions of the MSSM*, *Phys. Rev.* **D73** (2006) 115010, [hep-ph/0603247].

[42] M. Frank *et. al.*, *The Higgs boson masses and mixings of the complex MSSM in the Feynman-diagrammatic approach*, *JHEP* **02** (2007) 047, [hep-ph/0611326].

[43] F. Jegerlehner and A. Nyffeler, *The Muon g-2*, *arXiv:0902.3360* (2009) [arXiv:0902.3360].

[44] **Heavy Flavor Averaging Group** Collaboration, E. Barberio *et. al.*, *Averages of b−hadron and c−hadron Properties at the End of 2007*, *arXiv:0808.1297* (2008) [arXiv:0808.1297].

[45] M. Misiak *et. al.*, *The first estimate of B(anti-B –¿ X/s gamma) at O(alpha(s)**2)*, *Phys. Rev. Lett.* **98** (2007) 022002, [hep-ph/0609232].

[46] M. Artuso, E. Barberio, and S. Stone, *B Meson Decays*, *PMC Phys.* **A3** (2009) 3, [arXiv:0902.3743].

[47] A. J. Buras, P. H. Chankowski, J. Rosiek, and L. Slawianowska, $\Delta M_{d,s}, B^0 d, s \to \mu^+\mu^-$ *and* $B \to X_s\gamma$ *in supersymmetry at large* $\tan\beta$, *Nucl. Phys.* **B659** (2003) 3, [hep-ph/0210145].

[48] **WMAP** Collaboration, E. Komatsu *et. al.*, *Five-Year Wilkinson Microwave Anisotropy Probe (WMAP) Observations:Cosmological Interpretation*, *Astrophys. J. Suppl.* **180** (2009) 330–376, [arXiv:0803.0547].

[49] **CDMS** Collaboration, Z. Ahmed *et. al.*, *Search for Weakly Interacting Massive Particles with the First Five-Tower Data from the Cryogenic Dark Matter Search at the Soudan Underground Laboratory*, *Phys. Rev. Lett.* **102** (2009) 011301, [arXiv:0802.3530].

[50] J. R. Ellis, K. A. Olive, and C. Savage, *Hadronic Uncertainties in the Elastic Scattering of Supersymmetric Dark Matter*, *Phys. Rev.* **D77** (2008) 065026, [arXiv:0801.3656].

[51] E. A. Baltz, M. Battaglia, M. E. Peskin, and T. Wizansky, *Determination of dark matter properties at high-energy colliders*, *Phys. Rev.* **D74** (2006) 103521, [hep-ph/0602187].

[52] H. Baer, C. Balazs, A. Belyaev, T. Krupovnickas, and X. Tata, *Updated reach of the CERN LHC and constraints from relic density, b –¿ s gamma and a(mu) in the mSUGRA model*, *JHEP* **06** (2003) 054, [hep-ph/0304303].

[53] C. Balazs, M. S. Carena, and C. E. M. Wagner, *Dark matter, light stops and electroweak baryogenesis*, *Phys. Rev.* **D70** (2004) 015007, [hep-ph/0403224].

[54] C. Balazs, M. S. Carena, A. Menon, D. E. Morrissey, and C. E. M. Wagner, *The Supersymmetric Origin of Matter*, *Phys. Rev.* **D71** (2005) 075002, [hep-ph/0412264].

[55] A. Menon, D. E. Morrissey, and C. E. M. Wagner, *Electroweak baryogenesis and dark matter in the nMSSM*, *Phys. Rev.* **D70** (2004) 035005, [hep-ph/0404184].

[56] C. Balazs, M. S. Carena, A. Freitas, and C. E. M. Wagner, *Phenomenology of the nMSSM from colliders to cosmology*, *JHEP* **06** (2007) 066, [arXiv:0705.0431].

[57] D. S. Akerib *et. al.*, *The SuperCDMS proposal for dark matter detection*, *Nucl. Instrum. Meth.* **A559** (2006) 411–413.